



Manufacturing of cellulose-based paper: dynamic water absorption before and after fiber modifications with hydrophobic agents

A. Mohammadzadeh¹ · M. Barletta² · A. Gisario¹

Received: 3 March 2020 / Accepted: 20 April 2020 / Published online: 1 May 2020
© Springer-Verlag GmbH Germany, part of Springer Nature 2020

Abstract

Absorption of liquid or vapor water in paper designed for conversion processes is a critical phenomenon. In particular, the dimensional stability of the paper as the water content changes is crucial for the success of all the conversion processes, including copying and printing. Appropriate chemical treatments of the fibers can limit the phenomena of water absorption, allowing a better workability of the paper substrates. In the present study, moisture absorption tests were conducted under isothermal conditions on untreated papers and treated by coatings with silane, organo-siloxane and silicone agents, as well as with polyelectrolytes using layer-by-layer techniques. The treated and untreated papers were tested by changing the relative humidity between 0 and 80% relative humidity. The Guggenheim–Anderson–de Boer model was used to study moisture absorption isotherms, showing the increase in the dimensional stability of the papers after the chemical treatments of the fibers.

Keywords Cellulose · Dynamic water absorption · Dimensional stability · Fiber treatment · Manufacturing

1 Introduction

Absorption of water in wood–cellulosic materials occurs mainly through the fibers, the pores present between the fibers and the lumens inside the fibers [35]. When water interacts with cellulose, it causes physical alterations and dimensional changes in the fibers. An alteration in the moisture content of the paper can lead to a profound change in the geometric dimensions of the substrate and in the overall chemical–physical and mechanical properties [14]. The dimensional stability of the paper can be defined as its capability to resist deformations triggered by changes in temperature, humidity and pressure [42]. In general, dimensional stability usually indicates the resistance to deformation of the paper following a change in the moisture content and, in some cases, also following a change in temperature. Dimensional stability is commonly measured through

hygro-expansion tests [36], where expansion is measured as a function of the variation in the relative humidity of the material. The dimensional stability of the paper is dependent on the history of the transformation processes to which it has been subjected before. This result has been obtained in the past in Laroque [28], but more recently it has also been shown in Uesaka et al. [48], not only through absorption hysteresis tests, but also through specific tests of deformation under constrained conditions during which the paper is wet or subjected to a change in relative humidity [16].

Hygro-expansion of paper depends on a multitude of parameters relating to cellulose pulp and paper such as the type of wood pulp used in the manufacturing process, the shape of the fiber, the beating conditions of the fiber and orientation, pressure and stress acting on the fibers due to the drying phase [29, 31, 32]. The relationship between hygroscopic expansion in the plane and moisture content has been studied extensively in the past literature [5, 7, 18, 30, 38]. It has long been known that fiber deformation can be significantly reduced by cross-linking the fiber wall as reported in Cohen et al. [11] and Weatherwax and Caulfield [51], where formaldehyde was used to induce cross-linking in the fiber wall. Stamm [43] showed that cross-links can be also induced through a catalyzed heat treatment. More recently, the effect of fiber cross-linking on physical and mechanical

✉ M. Barletta
massimiliano.barletta@uniroma3.it

¹ Dipartimento di Ingegneria Meccanica e Aeronautica, Sapienza Università degli Studi di Roma, Via Eudossiana 18, 00184 Rome, Italy

² Dipartimento di Ingegneria, Università degli Studi Roma Tre, Via Vito Volterra 62, 00146 Rome, Italy

properties of the paper was studied in Horvath et al. [25] and Tejado et al. [45]. Oxidation is, for example, common to achieve fiber cross-linking, thus reducing significantly paper hygro-expansion [10]. The application of periodates is the most widespread technique, allowing to reduce hygro-expansion of at least 28% [20, 30]. Other techniques to improve the moisture resistance of paper involve chemical fiber treatments. In this respect, silanes have been used, for example, in large-scale applications as reported in Twomey et al. [47] and Gaiolas et al. [17]. Gaiolas et al. showed that grafting of two alkoxysilanes, namely vinyltrimethoxysilane and *g*-methacryloxypropyltrimethoxysilane, onto paper sheets by cold-plasma discharge leads to a reduction in the surface tension from about 29.3 to almost 0 mN/m. Tang et al. studied the influence of the fiber treatment with alkoxysilanes of different chain lengths (namely methyltrichlorosilane, butyltrichlorosilane, dodecyltrichlorosilane and octadecyltrichlorosilane) on the wetting properties of cellulose-based paper, showing the high resistance against oils of the octadecyltrichlorosilane-coated cellulose-based paper and the highest hydrophobicity of the methyltrichlorosilane-coated cellulose-based paper [44]. Silanes and siloxane resins are highly hydrophobic, with good resistance in the presence of humidity. Furthermore, these materials do not exhibit a toxicity profile for humans. Functionalization of cellulose-based paper aimed at generating liquid repellency was also investigated in the literature [9, 19] and, more recently, in Arslan et al. [4]. Combinations of anionic and cationic polyelectrolytes to hydrophobized cellulose-based papers were also widely investigated. More specifically, polyelectrolytes were used through the applications on the fibers of layer-by-layer (LbL) coatings, exploiting the anionic charge of the cellulose fiber. Decher [13], first, and Wagberg et al. [50], later, reported experimental studies in which the fibers were repeatedly treated with oppositely charged polyelectrolytes to form the multilayer. This technique allowed to obtain an excellent hydrophobization of the cellulose fibers. PEMs made of polyallylamine hydrochloride and polyacrylic acid applied to wood fibers were reported to lead to an increase in the number of fiber–fiber joints and in the number of covalent bonds in the contact area [15]. Contact angles greater than 90° were achieved by LbL techniques of polyallylamine (PAH) and polyacrylic acid (PAA), provided that the outermost layer was constituted by the cationic polyelectrolyte [21, 33].

Although the past research efforts, the significant results achieved and knowledge acquired, preservation of dimensional stability of converting paper is still an open topic, with scientists and practitioners still pushing toward the development of innovative and more effective solutions to protect paper by the effects of the water. In particular, the employment of hybrid silicone-based organic–inorganic resins to coat cellulose-based paper as well as the effect of the

additive concentrations on the fiber treatments is sparsely reported in the literature. The present work focuses, therefore, on the comparative evaluations of the ways by which as-is cellulose-based papers and papers treated with silane and siloxane agents used in different concentrations, with a silicone-modified resin or with polyelectrolytes through LbL techniques deform, when submitted to absorption of water vapor in isothermal conditions (at room temperature and for high humidity variations).

2 Materials and methods

2.1 Fibers (C)

As-is sheets (sample C) based on as-is cellulose without were prepared as follows: cellulose fiber with 243 g of short fiber (Cartiera di Guarcino SpA, Guarcino (FR), Italy), 27 g of long fiber (Cartiera di Guarcino SpA, Guarcino (FR), Italy) and 5 l of water were mixed in a pulper (Hitachi, Frank-PTI, Birkenau, Germany) for 10 min at 500 rpm. The mixture was transferred to the beating machine (Valley laboratory beater, Frank-PTI, Birkenau, Germany). The speed was at 600 rpm and additional 9 l of water was used for the refining process, which lasted 20 min. After beating, the fibers were drained, collected and stored in refrigerator.

2.2 Fiber modifications

As-is cellulose, that is, cellulose achieved as reported in Sect. 2.1, was mixed with different chemical agents in the homogenizer (Equalizer, Frank-PTI, Birkenau, Germany) at a constant speed of 150 rpm until homogenization was achieved.

2.2.1 Chemicals

2.2.1.1 Silane treatment (1DS and 2DS) 1 and 0.2% of volatile organic compound (VOC)-free waterborne silane (Dynasytan Sivo 121, Evonik Industries AG, Essen, Germany) was accurately mixed with 1 l of cellulose as previously obtained. The mixture was stirred for 2 h at 150 rpm. The Dynasytan Sivo 121 boasts a long-chain alkyl group which is highly hydrophobic. It also features a silanol group by which it can combine with the hydroxyl group of the cellulose-based substrate. By forming covalent bonds, the Dynasytan Sivo 121 is permeable to water vapor.

2.2.1.2 Oligosiloxane treatment (1DF and 2DF) 1 l of cellulose as previously achieved was mixed with 1 and 0.2% of fluoroalkyl-functional waterborne oligosiloxane (Dynasytan F8815, Evonik Industries AG, Essen, Germany) for 30 min at 150 rpm. Dynasytan F 8815 is a yellowish, slightly tur-

bid liquid. It acts as a surface modification agent on oxidic, carboxy- and hydroxy-functional substrates. In this case, Dynasylan F 8815 is combined by covalent bonds with the hydroxyl group of the cellulose-based substrate using the silanol groups. Hydrophobic properties are ensured by the fluoroalkyl functionality.

2.2.1.3 Siloxane treatment (12GF) 0.5% of polyether siloxane copolymer (Glide 450, Evonik Industries AG, Essen, Germany) was added to 1 l of cellulose as previously achieved and mixed in the homogenizer for 2 h at 150 rpm. TEGO® Glide 450 is a highly effective glide and flow additive with excellent compatibility. It is a clear liquid polyether siloxane copolymer. It can combine with the hydroxyl group of the cellulose-based substrate using the silanol groups. Addition of the product to the coating, can be as supplied or as a predilution. Predilution in a suitable solvent simplifies dosage and incorporation.

2.2.1.4 Silicone treatment (2S8) 1 l of cellulose as previously achieved was mixed with 2% of silicone-modified polyurethane dispersion (Silikopur 8080, Evonik Industries AG, Essen, Germany) for 30 min at 150 rpm. At the same time, 20% of Tego VariPlus DS 50 (Evonik Industries AG, Essen, Germany) was added to complete the chemical treatment. Silikopur 8080 combines the benefits of silicone resins with polyurethane polymers. It provides a water-beading effect and produces a slippery handle. It possesses extremely high flexibility and offers good recoatability and air-drying. It is water reducible and highly compatible. It can establish strong physical interaction with the cellulose-based substrates. TEGO® VariPlus DS 50 is an anionic dispersion of a polyurethane polyol resin for waterborne coatings and pigment concentrates delivered in liquid form. It improves adhesion on the substrate.

2.2.1.5 Polyelectrolyte multilayers (PAA/PAH) Polyallylamine hydrochloride (PAH, ABCR GmbH & Co, Karlsruhe, Germany) and polyacrylic acid (PAA, Sigma-Aldrich Corporation, St. Louis, Missouri) both in liquid form were used to build polyelectrolyte multilayers (LbL) on cellulose fibers. To optimize fiber adhesion, a solution of sodium chloride (NaCl) with a pH of 7.5 was used for the PAH layer and a solution of sodium chloride (NaCl) with a pH of 3.5 modified with hydrochloric acid (HCl) was used for the PAA layer. 100 g of cellulose, 500 g PAH, 500 g NaCl with 7.5 pH, 500 g PAA and 500 g NaCl with 3.5 pH were added. About 29.4 g of dried fiber pad was obtained by water drainage of 500 g of cellulose. LbL technique started with the addition of 29.4 g of the dried cellulose to 2.5 l of cationic PAH in the mixer at 150 rpm for 6 min. (Processing time and rotating speed of the mixer were constant.) The polyelectrolyte in excess was filtered, and the dried fiber pad

was rinsed with 2.5 l of NaCl solution with a pH of 7.5. The pad was re-suspended in 2.5 l of PAA and mixed for 6 min at 150 rpm. The pad was rinsed with 2.5 l of NaCl solution with a pH of 3.5. The process was repeated four times. At the end of the process, fibers treated with four-layer polyelectrolytes with a weight of 26 g were obtained. Adding 474 g of water, the treated fiber pad was ready for the hand-sheet process.

2.3 Hand-sheet forming process

Untreated and treated paper sheets were prepared using tap water in a Rapid-Kothen (Frank-PTI, Birkenau, Germany) hand-sheet former. After preheating untreated or treated samples in the Plexiglas container, the fiber suspension was filtered through a microporous bronze removable plate. One sample at a time was placed on the removable plate for the preparation of a sheet whose weight, thickness and average fiber radius were measured. The manufacturing of each individual sheet with different characteristics mentioned before was, then, carried out. The samples were placed in a dryer at 93 °C under a reduced pressure of 95 kPa for 5 min. Sheets with weights of 50 ± 10 g/m² were prepared. Finally, by setting the oven temperature at 94 °C for 10 min, post-curing of the fibers was promoted. The physical properties of untreated or treated sheets are given in Table 1.

2.4 Hygro-expansion tests

Contact angles were measured using a 30- μ l solvent droplet to wet the cellulose-based papers before and after the chemical treatments of the fibers. A tracer (blue methanol) was used to highlight the diffusion of the solvents on the samples surface. The images were captured using a high-speed digital camera in full HD with a resolution of 1920 \times 1280 pixels at a frame rate of (29.97, 25, 23.976 fps), shutter speed of 1/8000 s to 1/60 s and EF 100 mm f/2.8 Macro USM lens with focal length/aperture of 100 mm f/2.8, angle of view (diagonal: 24°, vertical: 14°, horizontal: 20°) and

Table 1 Physical properties of the samples

Sample	Weight (g)	Thickness (mm)	Mean fiber radius (μ m)
2DF	50 ± 10 g/m ²	0.1 ± 0.005 mm	6.80 μ m
2S8	50 ± 10 g/m ²	0.1 ± 0.005 mm	7.25 μ m
PAA/PAH	50 ± 10 g/m ²	0.1 ± 0.005 mm	8.75 μ m
C	50 ± 10 g/m ²	0.1 ± 0.005 mm	7.20 μ m
1DS	50 ± 10 g/m ²	0.1 ± 0.005 mm	9.41 μ m
2DS	50 ± 10 g/m ²	0.1 ± 0.005 mm	7.05 μ m
12GF	50 ± 10 g/m ²	0.1 ± 0.005 mm	7.10 μ m
1DF	50 ± 10 g/m ²	0.1 ± 0.005 mm	5.30 μ m

max magnification of $1.0\times$. The ImageJ program was used to measure the contact angles. A climatic room was used to obtain near-equilibrium absorption isotherms. A hygro-expansion test was, therefore, performed at the constant temperature of $25\text{ }^\circ\text{C}$ to determine both dimensional changes and moisture contents of each sample as a function of different relative humidity investigated. Each sample was placed in the climatic room and had an average starting weight of $50 \pm 10\text{ g/m}^2$ and a thickness of $0.1 \pm 0.005\text{ mm}$. The hygro-expansion process started with 0% relative humidity (RH) and ended with 80% relative humidity (RH). Every 10% increase in relative humidity during 24 h, the moisture content and dimensional movement of each sample were monitored and the results stored.

2.5 General assumptions

Absorption of a liquid droplet in a porous substrate is often described as a surface tension driven flow or wicking process. When an untreated, i.e., hydrophilic, paper comes into contact with liquid water, there is a rapid capillary absorption. In an ideal uniform capillary of length l , radius r and contact angle between the penetrating liquid and solid θ , the time to fill the capillary with a liquid (dynamic viscosity μ , surface tension γ) can be described by the integrated form of the Lucas–Washburn equation:

$$l = (r\gamma \cos \theta t / 2\mu)^{1/2}. \quad (1)$$

To evaluate the time dependency of the liquid penetration in the solid according to Eq. (1), Eq. (2) can be used:

$$l = kt^{1/2}. \quad (2)$$

A plot of l against $t^{1/2}$ is approximately a straight line with slope of $\sqrt{\left(\frac{r\gamma \cos \theta}{2\mu}\right)}$. $\sqrt{\left(\frac{r\gamma \cos \theta}{2\mu}\right)}$ is a measure of the penetrating power of a liquid in a solid, namely the coefficient of penetrance of the liquid. The Lucas–Washburn equation is based on the assumptions that all the capillaries have the same diameter. The capillaries do not connect to each other, and their length must be greater than their diameter. This equation describes the vertical absorption of a liquid into a relatively thick sheet. It does not account for any swelling of fibers or any other change in the porous structure of the substrate (i.e., paper). Absorption equilibrium is obtained when the number of molecules arriving on the surface is equal to the number of molecules leaving the surface.

The Guggenheim–Anderson–de Boer (GAB) model was developed independently by Guggenheim [1966], Anderson [2] and de Boer [12]. This model is based on the absorption theory of water on the surface of solids developed by BET [8]. The multi-parametric GAB model has been widely used

for the approximation of experimental data [49]. Equation (3) describes the GAB model:

$$u = \frac{mk \cdot C \cdot RH}{(1 - k \cdot RH)(1 - k \cdot RH + k \cdot C \cdot RH)} \quad (3)$$

$$C = De^{(H_m - H_c)/RT} \quad (4)$$

$$k = Be^{(H_c - H_n)/RT} \quad (5)$$

where u is the fractional moisture content % at equilibrium; m , monolayer moisture content, i.e., concentration of primary active surface sites; C , kinetic constant related to the sorption in the first layer; k , kinetic constant related to multi-layer sorption, i.e., factor correcting properties of multilayer with respect to bulk liquid; RH , relative humidity; H_m , H_n and H_c molar sorption enthalpies of the monolayer, multi-layer and heat of condensation of water, respectively; R , gas constant $\frac{\text{N}\cdot\text{m}}{\text{mol}\cdot\text{K}}$; T , absolute temperature; and D and B , entropic accommodation factors.

Equation (5) can be also rewritten as:

$$\frac{RH}{u} = \alpha RH^2 + \beta RH + \gamma \quad (6)$$

where

$$a' = \frac{k}{m} \left(\frac{1}{C} - 1 \right) \quad (7)$$

$$a'' = \frac{1}{m} \left(1 - \frac{2}{C} \right) \quad (8)$$

$$a''' = \frac{1}{mkC}. \quad (9)$$

The GAB model is, therefore, a three-parameter model, with equilibrium moisture content that can be regressed using Eq. (6) by the three coefficients a' , a'' and a''' . Once evaluated the coefficients, the values of the parameter, m , k and C can be calculated accordingly.

Stability of a paper ε is often quantified through hygro-expansion in tests that involve humidity changes:

$$\varepsilon = \frac{\Delta l}{l}. \quad (10)$$

It is often related to the change in moisture content (ΔMC) or relative humidity (ΔRH) as a hygro-expansion coefficient:

$$\beta = \frac{\varepsilon}{\Delta MC \text{ or } \Delta RH}. \quad (11)$$

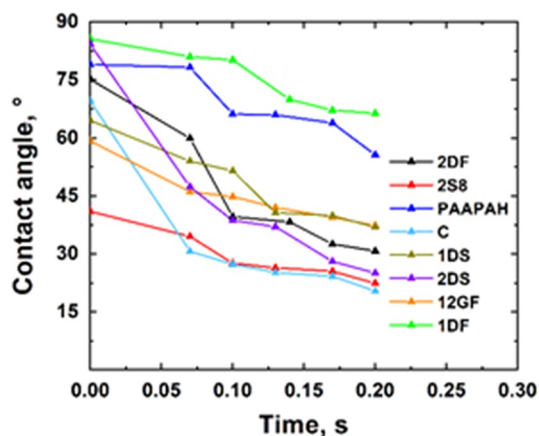


Fig. 1 Contact angle as a function of time for a water droplet with an initial size 30 μL for treated and untreated samples

3 Results and discussion

Figure 1 shows the trend of the contact angle between a water droplet and the cellulose-based papers before and after the different chemical treatments. The samples treated with 1DF and PAA/PAH show values of the contact angles with time always higher than 60°. The samples 1DF or PAA/PAH exhibit the highest contact angle both at the beginning and at the end of the test. This result is probably attributed to a reduction in the content of hydroxyl groups and a significant increase in cross-linking of the paper sheets caused by the chemical treatment with the additives, that is, the hydrophobic fluoroalkyl-functional oligosiloxane (1DF) and the PAA/PAH multilayer. Conversely, the samples 2S8 (the silicone-based resin), 2DS and 2DF show the lowest contact angles (always lower than 45 °C), and after a short time range (i.e., <0.1 s), the contact angles approach ~30°, the same value found on the as-is cellulose-based paper. The lowest contact angles found for the samples 2DS and 2DF can be probably ascribed to the lower additive concentrations used during the fiber treatment. The lowest angle found for the sample 2S8 can be, instead, ascribed to the presence of hydroxyl functionality on the hybrid resin, which makes it quite hydrophilic.

Isothermal water vapor absorption experiments were performed to test the mechanisms behind the dynamic absorption of water in samples 0.1 mm thick, when they are submitted to broad changes in relative humidity (RH). The results were estimated as weight change, thus allowing to measure the moisture content (MC) of the samples. This type of investigation is also called step-response analysis. The differences in sorption properties between the different samples investigated can be illustrated by the sorption isotherms shown in Fig. 2. The weight of the samples was registered every 24 h under temperature control and the step-by-step

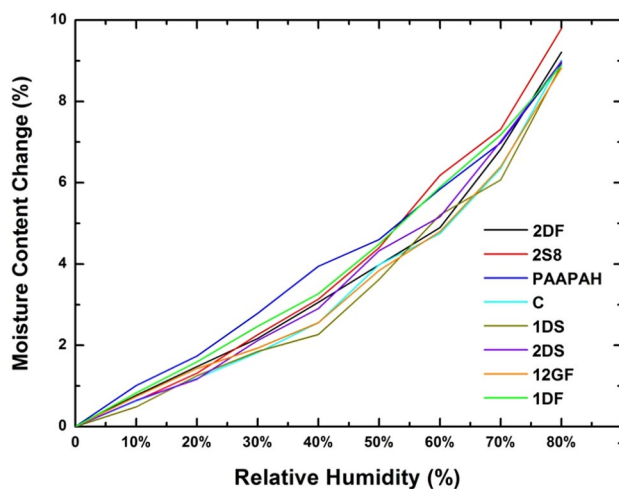


Fig. 2 Sorption in isothermal conditions for treated and untreated paper sheets

change in relative humidity. The temperature was 25°C and the relative humidity varied from 0 to 80% RH during the experimental tests. The results of the step-response analysis were partly given as gravimetric moisture content and, then, normalized as non-dimensional moisture content of the sample $0 < u < 10%$, as determined by Eq. (12):

$$u = \frac{m_t - m_0}{m_0} \tag{12}$$

where m_t is the moisture content at time t and m_0 is the moisture content at $t=0$. Observing the experimental data of the sorption isotherms reported in Fig. 2, the water content is, as expected, related to the relative humidity according to a sigmoidal relationship according to the classification by Brauner [6]. This type of absorption isotherms matches well with the GAB model. GAB model is based on three mechanisms of absorption [1], that is, (1) monomolecular absorption; (2) multilayer absorption with the heat of absorption greater than the vapor heat of condensation; and (3) multilayer absorption with the heat of absorption equal to or less than the vapor heat of condensation. Moisture absorption isotherms for all the investigated samples at 25 °C are shown in Fig. 3. The fitting by the GAB models for the 2DF sample according to Eq. (9) is also highlighted:

$$u = \frac{m \cdot k \cdot C \cdot RH}{(1 - k \cdot RH)(1 - k \cdot RH + k \cdot C \cdot RH)} \tag{13}$$

Moisture has a significant effect on the physical properties of paper sheets leading to dimensional changes. There are two mechanisms that control the interaction of moisture with paper, when relative humidity changes [27]. The first mechanism is the equilibrium sorption capacity of a paper sheet described by the moisture sorption isotherm [26]. This

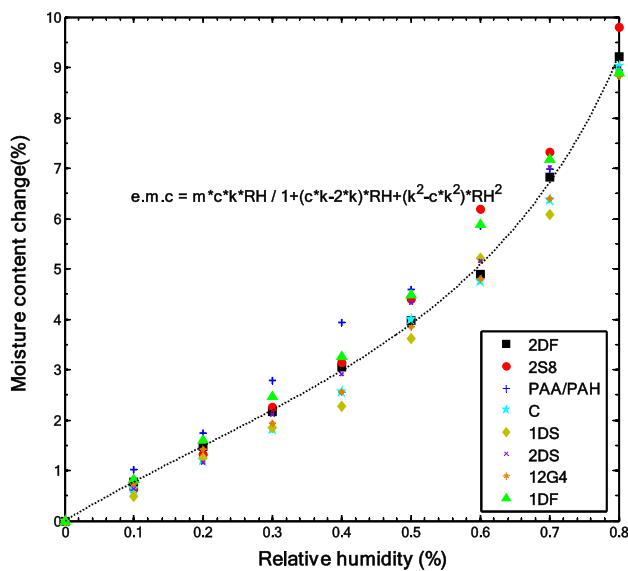


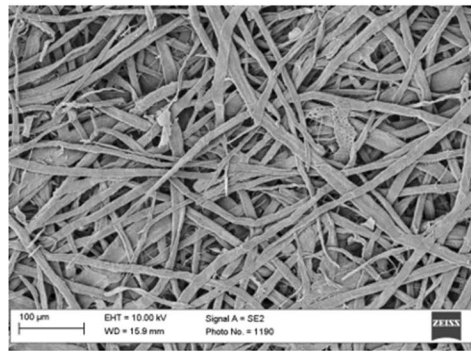
Fig. 3 Moisture sorption behavior and fitting by the GAB model

obviously determines the ultimate moisture content of the paper sheets as well as their limited response to a change in humidity, when transport resistance is negligible. The second mechanism is the nature of transport resistance of the paper sheets [37]. Transport resistance can be characterized by the transport of moisture through the paper sheet under steady-state conditions. The interaction between these two mechanisms gives the transient response of paper sheets under changing humidity conditions. The equilibrium of moisture absorption behavior of paper is like that of other cellulosic materials. Since the cellulose material is hygroscopic and porous, in view of this high hygroscopicity, the paper can absorb water vapor from the environment, which can cause the loss of its original properties. On the other hand, due to the heterogeneity of porous material, moisture diffusion can occur via two pathways [39]: the void spaces and the fiber matrix. Since the void structure in paper and the fiber matrix are anisotropic, diffusion is also anisotropic. Therefore, the definition of lateral diffusion in the plane of the paper sheets (xy) and transversal diffusion in the thickness direction (z) is perfectly in accordance with the GAB equation. Figure 4 reports the SEM images of the different samples herein investigated. Due to the typical sheet production process, fibers are mostly aligned in the machine direction (MD). The expansion of single fibers is notoriously higher in the transverse direction than in the longitudinal direction. The expansion of paper in cross direction (CD) is, therefore, up to seven times higher than in the machine direction (MD), as reported in Figueiredo et al. [16]. In the present papermaking process, there is no orientation, namely the fiber orientation is in-plane isotropic. Under this circumstance, the sheet hygro-expansion can be expected to

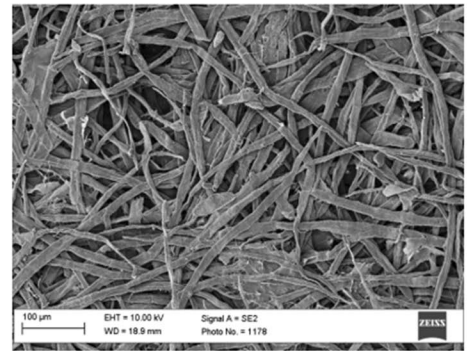
correlate with the transverse fiber expansion in both directions [40]. It is possible to notice, in fact, the random and anisotropic distribution of the fibers before and after the treatments for all the samples, regardless of the chemical additives involved in the experimental tests or their concentration in the mixture. In addition, the cellulose fibers involved in the preparation of the samples were always the same (243 g of short fiber combined with 27 g of long fiber). However, the relation between hygro-expansion and fiber length, width and wall thickness is generally controversial as summarized in Lindner [32]. Fibers curl (ratio between the fiber contour length and the longest dimension of the fiber) and shape factor (ratio between the longest dimension of the fiber and fiber contour length) also can play a certain role, as they influence significantly the inter-fibers contact [3]. In this case, the samples were manufactured using the same papermaking process, using the same fibers. For this reason, no differences in hygro-expansion, apart from the different additive used to modify the fibers, are expected from the fibers type or by the production process. Density and fiber content are seen to be almost the same in Fig. 4. The only differences between the samples investigated can, therefore, reside in the type of inter-fiber contacts and fiber porosities that are obviously affected by the chemical treatments of the fibers themselves.

The GAB parameters for all the investigated samples, the coefficient of determination R^2 and the root-mean-square-error ($RMSE$) are given in Table 2. In general, the GAB model fits the experimental isotherm data with a great deal of accuracy. In the present experiments, the values of GAB parameters (m , the monolayer capacity, i.e., concentration of primary active surface sites; C , the kinetic constant related to the absorption in the first layer; k , the kinetic constant related to multilayer absorption) are in the range of 3–4 for m , 1.3 for C and 0.8–0.9 for k . Compared to untreated samples, the values of m decreased after chemical treatments of the fiber networks, except for the 2DF and 2S8 treatments. The reduction in the monolayer capacity (i.e., of the m value) of most of the treated samples is consistent with the reduction in the hydrophilic character of the treated surface after chemical modifications, especially for the samples 1DF, 1DS and 12GF. In PAA/PAH, 1DF, 1DS and 12GF samples, the parameters of the GAB model C , related to the kinetic constant of the sorption in the first layer, and k , related to the kinetic constant of the multilayer absorption, were decidedly small. The analysis of these constants indicates that the modification of the cellulose by the selected chemical treatments leads to a significant decrease in the formation of hydrogen bond in the first layer and in the multilayer structure of these samples, slowing water sorption. This result might be attributed to the pore orientation and to the lack of hydrophilic sites at the fiber surface after the chemical treatments. In contrast, the increase in the parameter m in

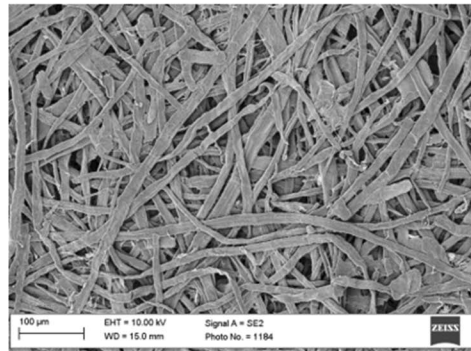
Fig. 4 SEM micrographs showing the cellulose fibers before and after treatments



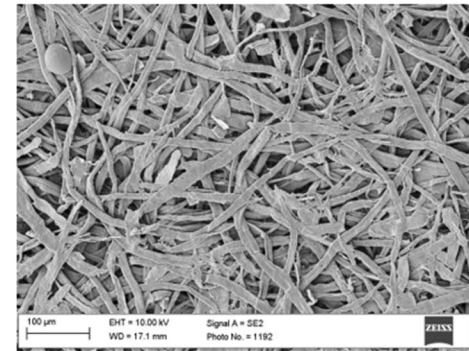
1DF sample



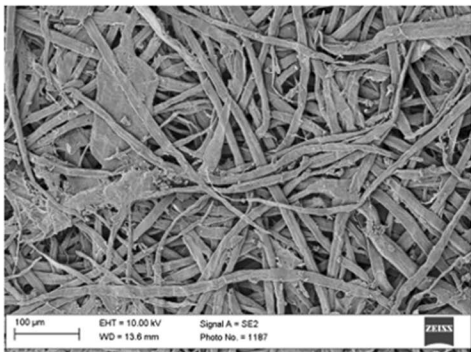
1DS sample



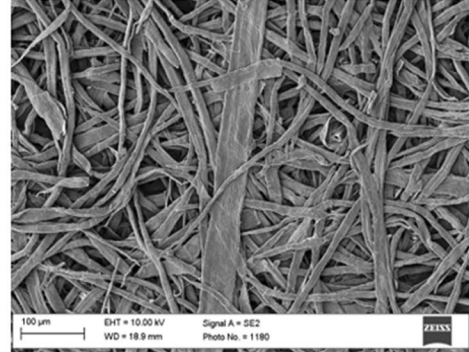
2DF sample



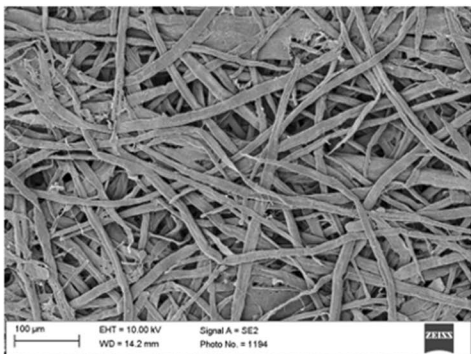
2DS sample



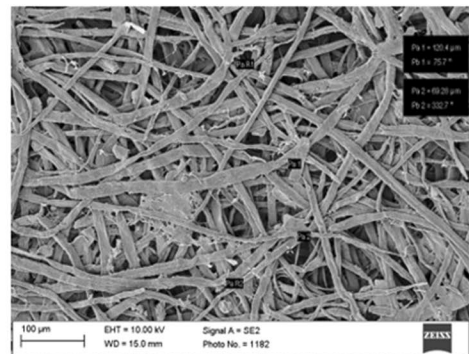
2S8 sample



12GF sample



C sample



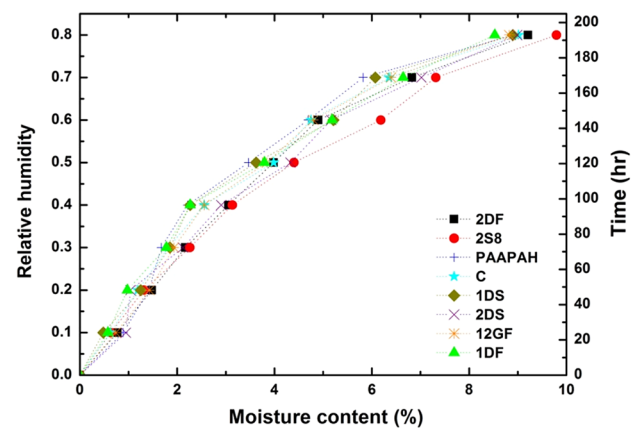
PAAPAH sample

Table 2 GAB parameters obtained from sorption isotherms at 25 °C

Sample	<i>C</i>	<i>k</i>	<i>m</i>	<i>R</i> -square
2DF	2.282	0.8510	3.621	0.9986
2S8	2.689	0.8522	3.712	0.9935
PAA/PAH	1.711	0.8420	3.579	0.9933
C	2.154	0.8482	3.615	0.9970
1DS	1.997	0.8420	3.568	0.9950
2DS	2.450	0.8432	3.581	0.9959
12GF	2.057	0.8425	3.550	0.9983
1DF	2.011	0.8410	3.540	0.9923

the samples C, 2DF, 2S8 and 2DS can be explained by the presence of hydroxyl units that make the samples hydrophilic, since their hydrogen active group can interact with the moisture through the onset of hydrogen bonds. The isothermal absorption tests also show that the moisture content for the samples 1DF, 12GF, 1DS and PAA/PAH, calculated at 80% relative humidity (25 °C) using the GAB equation, was 8.76, 8.77, 8.84 and 9% of water grams per grams of dry solid, respectively. The increase in monolayer capacity of these samples, that is, in the value of parameter *m*, can be associated with the increase in moisture content at 80% relative humidity. The steady-state moisture diffusion through paper can be explained, in this case, as a combined process between the water vapor diffusion through the fiber pores and bound water diffusion through the fiber walls [39]. Different pore characteristics can be inferred for open-pore structures in lateral and transverse direction after treatment of cellulose fibers with the different chemical agents herein investigated. The transverse pore size distribution can be broader than in other directions, thus favoring the anisotropic diffusion in paper in agreement with the results of Topgard and Soderman [46]. Therefore, the flow in the transverse direction encounters a pore structure that should be much more open than in the lateral direction. The low value of the parameter *m*, that is, of the monolayer capacity, for the samples 1DF, 12GF, 1DS and PAA/PAH compared to other samples might be explained by the low rate of diffusion in the transverse direction for these samples. Surface diffusion was thought to dominate only after the fiber surface was covered with a monolayer of absorbed molecules. The molecules constituting the monolayer are thought to be chemically bound and cannot diffuse easily. This would explain why the exchange between water vapor in the paper pores and bound water in the fiber surface is much faster than the moisture diffusion in the thickness direction. Accordingly, the low value of *k* for all the samples shows that the kinetic constant related to multilayer absorption is smaller than the kinetic constant related to the absorption in the first layer *C*.

Figure 5 shows the trend of relative humidity with testing time and moisture content for all the investigated samples,

**Fig. 5** Trend of relative humidity with testing time and moisture content

when submitted to a change in relative humidity from 0 to 80% RH. With *HR* around 10% and after 24 h, the moisture content of the samples 2DS, 2DF, 2S8 and of the untreated sample C increased the most. After the increase in *HR* to 40%, the 2DS, 2DF and 2S8 samples showed further significant increase in moisture content. Fiber modification using 1DF and 1DS leads to slower increase in moisture content, which agrees with the kinetic constant *k* of the multilayer absorption in the GAB model. These values were 0.8410 and 0.820% g water/g dry solid, respectively. When the samples were in equilibrium at 80% RH, the 2DF, 2S8, C and 2DS showed the highest moisture content. These results are in agreement with Singha and Rana [41], where a reduction in moisture uptake and a reduction in paper sheet swelling were observed by fiber modification with organic, prevalently hydrophobic, constituents. Table 3 displays the fit of the GAB model with the experimental data. The samples 2DF, 2DS, 2S8 and the untreated sample C have, as a common effect, to noticeably increase the water vapor absorption in the fibers in the whole relative humidity range, in

Table 3 Dimensional change (ϵ), change in moisture content (ΔMC) and hygro-expansion coefficient (β)

Sample	Expansion (%)	Change in moisture content (%)	Hygro-expansion coefficient (%/%)
2DF	0.6691	7.3366	0.0912
2S8	0.6791	7.3671	0.0921
PAA/PAH	0.6386	7.1047	0.0898
C	0.6632	7.3146	0.0906
1DS	0.5876	6.9208	0.0849
2DS	0.6594	7.2925	0.0904
12GF	0.5436	6.7602	0.0804
1DF	0.5437	6.6305	0.0820

Values are taken in sorption tests from 30 to 80% RH

accordance with the constant values of the GAB model. The capacity of the monolayer m , the kinetics of absorption in the first layer C and the kinetic constant related to multilayer sorption k were considerably higher for these samples. This effect has been partly attributed to the appearance of a fraction of the hydrophilic sites at the fiber surface and, possibly, at the transverse and lateral direction of the water diffusion because of the chemical treatments in agreement with Gupta and Chatterjee [23, 24]. The analysis of water vapor absorption kinetics of untreated and treated samples indicates, therefore, that: (1) the variation of the water vapor diffusion coefficient versus relative humidity complies with the GAB model hypothesis; (2) water vapor is probably more mobile in the first layer compared to multilayer absorption for all samples; (3) the diffusivity of moisture clearly decreased due to the different chemical treatments, as occurred for the samples 1DF, 1DS and 12GF, because of the disappearance of a fraction of the hydrophilic sites and bound water.

The dimensional stability was measured on the treated and untreated samples by exposing them to humidity cycles between 30 and 80% RH. The dimensional change (moisture content at 80% RH – moisture content at 30% RH) reported in Fig. 6 was calculated to achieve the hygro-expansion coefficient β described in Eq. (7) and is shown in Table 3. The hygro-expansion coefficient in the samples 1DF, 1DS and 12GF was lower than in untreated C and 2S8 treated samples, together with those treated by chemical agents at lower concentration (2DS and 2DF samples). This coefficient for the PAA/PAH sample was higher than for the 1DF, 1DS and 12GF samples, but less than for the other samples. As previously seen, there is a significant inter-fiber contact area in the 1DF, 1DS, 12GF and PAA/PAH samples compared with the untreated sample and the samples treated by chemical agents at lower concentration (2DS and 2DF samples). No major differences in dimensional

changes were, instead, observed between the samples 2DF, 2DS, 2S8 and the untreated sample C, as shown in Table 3. Therefore, increasing the adhesion properties between fibers by the chemical treatment has a significant influence on the dimensional stability of paper and, as a result, they can show a lower expansion coefficient β . These results are in agreement with the aforementioned experimental findings reported in Singha and Rana [41] as well as with results about PEM reported in Larsson and Wågberg [29], where the reduction in dimensional change was reduced after grafting of the fibers with organic or hybrid organic–inorganic constituents or after LbL deposition with polyelectrolytes. It can be concluded that, in agreement with the recent findings in Lindner [32], the inter-fiber contact significantly affects the paper sheet hygro-expansion coefficient. Figure 7 shows the trend of the dimensional change as a function of moisture content for the samples exposed to variable relative humidity from 30 to 80%. At 40% RH, the moisture content of the 2DF, 2S8, C and 2DS samples was higher than those of other samples, with the difference that 2DS also showed higher-dimensional changes. The samples PAA/PAH, 1DF, 12GF and 1DS exhibited, instead, lower moisture content and dimensional change, but the dimensional change in the sample 1DS was higher compared to the others. With the increase in relative humidity to 50%, the behavior of all the samples did not change. This result indicates that the fibers modified by PAA/PAH, 1DF and 12GF treatments had lower water absorption capacity than other samples. The reason can be the enhanced adhesion between the fibers (i.e., higher inter-fiber contact) by the treatment. At approximately 60% relative humidity, the dimensional change decreased rapidly in the 1DS and 1DF samples. The PAA/PAH and 12GF samples showed lower moisture content with the increase in dimensional change compared to 1DF and 1DS samples.

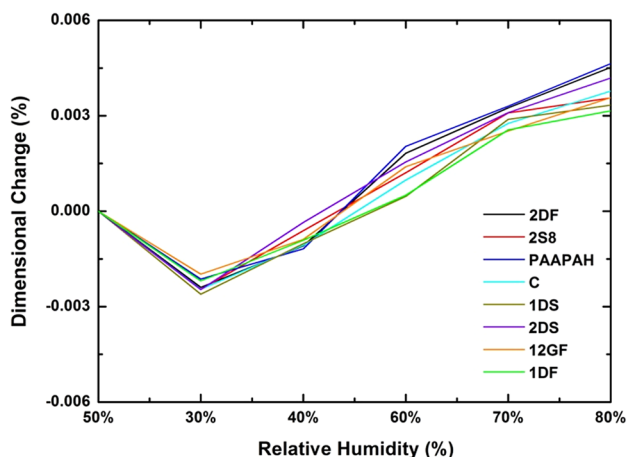


Fig. 6 Trend of dimensional changes with relative humidity

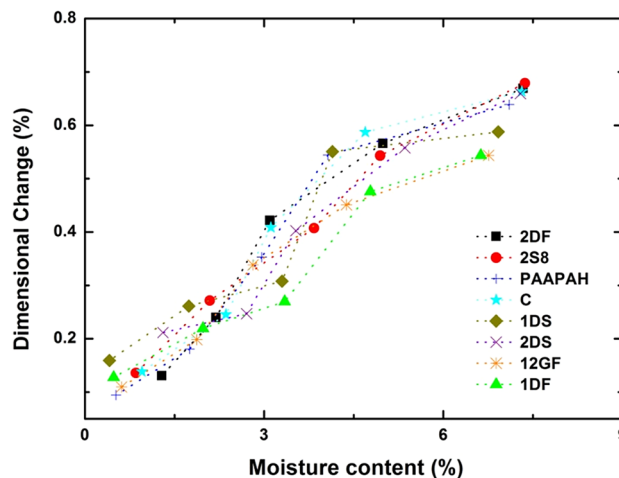


Fig. 7 Trend of hygro-expansion with moisture content. Values are taken in sorption tests from 30 to 80% RH

The samples 2S8 and 2DS reached a higher moisture content. The sample 2DF and the untreated sample C had a higher-dimensional change than other samples. The moisture content of these samples was significantly lower than that of the 2S8 and 2DS samples. At 70% relative humidity, the samples PAA/PAH and 1DS were characterized by a significant increase in the dimensional change. For samples 12GF and 1DF, the dimensional change was lower than that found for the PAA/PAH and 1DS samples. The moisture content for these samples was nearly constant. The other samples showed no differences between 60 and 70% RH. Slow absorption or unexpected dimensional changes for the investigated samples under different values of relative humidity can be probably related to the different types of amorphous and crystalline regions that characterize each sample, external or internal fiber surfaces and direct or indirect absorption as reported in Gupta and Chatterjee [23, 24]. Water vapor molecules are absorbed directly on the hydroxyl groups of the external surface, amorphous regions, inner surface of voids and crystallites of the samples. Additional water vapor molecules can be absorbed in the water molecules binding the fiber directly. The direct absorption of the water molecules into the external surface and amorphous regions is generally considered to occur very fast, while the indirect absorption in the inner surface and crystallites take often place in a relatively slow fashion [34]. At 80% relative humidity, the samples 1DF and 12GF showed a lower moisture content with lower-dimensional change. The sample 1DS also showed the same behavior, but the dimensional change was even higher. For the sample PAA/PAH, the dimensional change was also higher than those found for 1DF, 12GF and 1DS. The samples 2S8, 2DF, C and 2DS had a high level of moisture content and dimensional change. During the absorption tests, as a matter of fact, all the samples exhibited unstable properties when the relative humidity of the environment was progressively increased.

4 Conclusions

In the present work, untreated and chemically treated (i.e., fibers sized by the addition of silane, siloxane, silicone and fiber sized by deposition of polyelectrolytes according to layer-by-layer (LbL) technique) paper sheets were exposed to cyclic step (relative humidity) RH changes in climatic chamber under strictly controlled operating conditions. The moisture sorption isotherms for untreated and chemically treated paper sheets at 25 °C were investigated and interpreted in light of the multi-parametric GAB model. Experimental data show that the chemical treatments of paper sheets result in an often significant reduction in the water absorption in the fibers and in the corresponding dimensional change, with this result being mostly

ascribable to the modification between the inter-fiber contacts. The results follow the GAB model with good accuracy. They indicate that a decrease in the hydrophilic sites at the fiber surface, as occurred for the samples 1DF, 1DS, 12GF and PAA/PAH, leads to a significant decrease in the hygro-expansion coefficient and, accordingly, in the reduction in monolayer capacity and in the kinetic constants relating to the first and multilayer absorption sites. In addition, the chemical treatment effects were stronger for the samples 1DF, 1DS, 12GF and PAA/PAH than for the others due to their higher inter-fiber contacts and adhesion that made the fiber network decidedly more stable.

References

1. M. Alam, N. Islam, Study on water sorption isotherm of summer onion. *Bangladesh J. Agric. Resour.* **40**(1), 35–51 (2015)
2. R.B. Anderson, Modification of the B.E.T. equation, *J. Am. Chem. Soc.* **68**, 686–691 (1946)
3. S. Antonsson, P. Makela, C. Fellers, M. Lindstrom, Comparison of the physical properties between hardwood and softwood pulps. *Nord. Pulp Pap. Res. J.* **24**(4), 409–414 (2009)
4. O. Arslan, Z. Aytac, T. Uyar, Superhydrophobic, hybrid, electrospun cellulose acetate nanofibrous mats for oil/water separation by tailored surface modification. *ACS Appl. Mater. Interfaces.* **8**(30), 19747–19754 (2016)
5. C. Brandon, *Dimensional Stability in Pulp and Paper Chemistry and Chemical Technology*, vol. 3 (Wiley Inc., New York City, 1980)
6. S. Brauner, *The Absorption of Gases and Vapors*, vol. 1 (Oxford University Press, Oxford, 1943)
7. W. Brecht, Beating and hygrostability of paper, in *Fundamentals of Papermaking Fibres. Beating and Hygrostability of Paper*, ed. by F. Bolam (L. B. Association, A cura di, Cambridge, UK, 1958), pp. 241–262
8. S. Brunauer, P. Emmett, E. Teller, Adsorption of gases in multimolecular layers. *J. Am. Chem. Soc.* **60**, 309–319 (1938)
9. L. Chen, A. Geisser, E. Bonaccorso, K. Zhang, Transparent slippery surfaces made with sustainable porous cellulose lauroyl ester films. *ACS Appl. Mater. Interfaces.* **6**(9), 6969–6976 (2014)
10. Y. Chung, P.-K. Pak, Effect of crosslinking on dimensional stability and dyeability of Korean traditional paper. *Text. Sci. Eng.* **43**(2), 95–100 (2006)
11. W. Cohen, A.J. Stamm, D.J. Fahey, Dimensional stabilization of paper by catalyzed heat-treatment. *Tappi J.* **42**, 904–908 (1959)
12. J.H. de Boer, *The Dynamical Character of Adsorption* (Clarendon Press, Oxford, UK 1953)
13. G. Decher, Fuzzy nano-assemblies: toward layered polymeric multicomposites. *Science* **277**(5330), 1232–1237 (1997)
14. S. Elyasi, H. Torshizi, Concentration of anionic starch solution in paper surface sizing on physical and strength properties of recycled paper. *Iran. J. Wood Pap. Ind.* **7**(4), 487–497 (2017)
15. M. Eriksson, A. Torgnysdotter, L. Wagberg, Surface modification of wood fibers using the polyelectrolyte multilayer technique: effects on fiber joint and paper strength properties. *Ind. Eng. Chem. Res.* **45**(15), 5279–5286 (2006)
16. A. Figueiredo, S. Magina, D. Evtuguin, E. Cardoso, J. Ferrá, P. Cruz, Factors affecting the dimensional stability of decorative papers under moistening. *BioResources* **11**(1), 2020–2029 (2016)

17. C. Gaiolas, A. Costa, M. Nunes, M. Silva, M. Belgacem, Grafting of paper by silane coupling agents using. *Plasma Processes Polym.* **5**(5), 444–452 (2008)
18. W. Gallay, Stability of dimensions and form of paper. *Tappi J.* **56**(11), 54–63 (1973)
19. A. Geissler, L. Chen, K. Zhang, E. Bonaccorso, M. Biesalski, Superhydrophobic surfaces fabricated from nano- and microstructured cellulose stearoyl esters. *Chem. Commun.* **49**, 4962–4964 (2013)
20. M. Gimaker, *Influence of fibre modification on moisture sorption and the mechanical properties of paper* (KTH Royal Institute of Technology, Department of Fibre and Polymer Technology, Division of Fibre Technology, Stockholm, Sweden, 2010)
21. V. Gribova, R. Auzely-Velty, C. Picart, Polyelectrolyte multilayer assemblies on materials surfaces: from cell adhesion to tissue engineering. *Chem. Mater.* **24**(5), 854–869 (2012)
22. E.A. Guggenheim, *Applications of Statistical Mechanics*, (Clarendon Press, Oxford, UK, 1966)
23. H. Gupta, S. Chatterjee, Parallel diffusion of moisture in paper. Part 1: steady-state conditions. *Ind. Eng. Chem. Res.* **42**(25), 6582–6592 (2003)
24. H. Gupta, S. Chatterjee, Parallel diffusion of moisture in paper. Part 2: transient conditions. *Ind. Eng. Chem. Res.* **42**(25), 6593–6600 (2003)
25. A. Horvath, R. Pelton, P. Larsson, L. Wagberg, Effect of cross-linking fiber joints on the tensile and fracture. *Ind. Eng. Chem. Res.* **49**(14), 6422–6431 (2010)
26. A. Khan, Theory of adsorption equilibria analysis based on general equilibrium constant expression. *Turk. J. Chem.* **36**, 219–231 (2012)
27. A. Khazraji, R. Sylvain, Interaction effects between cellulose and water in nanocrystalline and amorphous regions: a novel approach using molecular modeling. *J. Nanomater.* **2013**, @409676@@ (2013)
28. G. Laroque, The extension of paper by absorbed water vapor. *Pulp Pap. Mag. Can.* **37**, 199–209 (1936)
29. P. Larsson, L. Wågberg, Influence of fibre–fibre joint properties on the dimensional stability of paper. *Cellulose* **15**(4), 515–525 (2008)
30. P. Larsson, M. Gimaker, L. Wagberg, The influence of periodate oxidation on the moisture sorptivity and dimensional stability of paper. *Cellulose* **15**, 837–848 (2008)
31. P. Larsson, M. Hoc, L. Wagberg, The influence of grammage, moisture content, fibre furnish and chemical modifications on the hygro- and hydro-expansion of paper, in *14th Fundamental Research Symposium on Advances in Pulp and Paper Research* (St Annes Coll, Oxford, England, 2009) pp. 355–388
32. M. Lindner, Factors affecting the hygroexpansion of paper. *J. Mater. Sci.* **53**, 1–26 (2018)
33. R. Lingstrom, S. Notley, L. Wagberg, Wettability changes in the formation of polymeric multilayers on cellulose fibres and their influence on wet adhesion. *J. Colloid Interface Sci.* **314**(1), 1–9 (2007)
34. V. Lovikka, L. Rautkari, T. Maloney, Changes in the hygroscopic behavior of cellulose due to variations in relative humidity. *Cellulose* **25**(1), 87–104 (2018)
35. H. Modaressi, G. Garnier, Mechanism of wetting and absorption of water droplets on sized paper: effects of chemical and physical heterogeneity. *Langmuir* **18**(3), 642–649 (2002)
36. W. Obeid, A. Alliche, G. Mounajed, Identification of the physical parameters used in the thermo-hygro-mechanical model. *Transp. Porous Media* **45**, 215–239 (2001)
37. S. Pekka, *Studies of water transport in paper during short contact* (Laboratory of Paper Chemistry, Department of Chemical Engineering, Abo Akademi, Turku, Finland, 1988)
38. I. Pulkkinen, J. Fiskari, V. Alopaeus (2009), The effect of sample size and shape on the hygroexpansion coefficient—a study made with advanced methods for hygroexpansion measurement. Technical Association of the Pulp and Paper Industry of Southern Africa (2009), pp. 26–33
39. B. Ramarao, A. Massoquete, S. Lavrykov, S. Ramaswamy, Moisture diffusion inside paper materials in the hygroscopic range and characteristics of diffusivity parameters. *Dry. Technol.* **10**(10), 2007–2056 (2003)
40. W. Sampson, J. Yamamoto, The drying shrinkage of cellulosic fibres and isotropic paper sheets. *J. Mater. Sci.* **46**(2), 541–547 (2011)
41. A. Singha, R. Rana, Effect of pressure induced graft copolymerization on the physico-chemical properties of bio-fibers. *BioResources* **5**(2), 1055–1073 (2010)
42. J. Songok, P. Salminen, M. Toivakka, Temperature effects on dynamic water absorption into paper. *J. Colloid Interface Sci.* **418**, 373–377 (2014)
43. A. Stamm, Dimensional stabilisation of wood by catalysed heat treatment and crosslinking with formaldehyde. *Tappi J.* **42**(1), 39–44 (1959)
44. Z. Tang, H. Li, D. Hess, V. Breedveld, Effect of chain length on the wetting properties of alkyltrichlorosilane coated cellulose-based paper. *Cellulose* **23**, 1401–1413 (2016)
45. A. Tejado, M. Antal, X. Liu, T. van de Ven, Wet cross-linking of cellulose fibers via a bioconjugation reaction. *Ind. Eng. Chem. Res.* **50**(10), 5907–5913 (2011)
46. D. Topgard, O. Soderman, Diffusion of water absorbed in cellulose fibers studied with 1H-NMR. *Langmuir* **17**(9), 2694–2702 (2001)
47. B. Twomey, D. Dowling, G. Byrne, L. O’Neill, L. O’Hare, Properties of siloxane coatings deposited in a reel-to-reel atmospheric pressure plasma system. *Plasma Processes Polym.* **4**(S1), S450–S454 (2007)
48. T. Uesaka, I. Kodaka, S. Okushima, R. Fukuchi, History-dependent dimensional stability of paper. *Rheol. Acta* **28**(3), 238–245 (1989)
49. R. Villalobos, P. Hernandez, E. Teller, Effect of surfactants on water sorption and barrier properties of hydroxypropyl methylcellulose films. *Food Hydrocolloids* **20**, 502–509 (2006)
50. L. Wagberg, S. Forsberg, A. Johansson, P. Juntti, Engineering of fibre surface properties by application of the polyelectrolyte multilayer concept. Part I: modification of paper strength. *J. Pulp Pap. Sci.* **28**(7), 222–228 (2002)
51. R. Weatherwax, D. Caulfield, The pore structure of papers wet stiffened by formaldehyde crosslinking: I. Results from the water isotherm. *J. Colloid Interface Sci.* **67**(3), 498–505 (1978)

Publisher’s Note Springer Nature remains neutral with regard to jurisdictional claims in published maps and institutional affiliations.